

#### Published by Avanti Publishers

# Journal of Advances in Applied & Computational Mathematics

ISSN (online): 2409-5761



## A Mathematical Model for the Saturation Effects of Radiotherapy with Oscillating Tumor Density

G.V.R.K. Vithanage <sup>1</sup>,\*, A.R.M. Hasini Parami Wattetenne <sup>1</sup>, K.A. Nirupadhi Divyanjali Jayakody <sup>1</sup>, M. Sawani Dhanushika <sup>1</sup> and Sachith Dassanayaka <sup>1</sup>

#### **ARTICLE INFO**

Article Type: Research Article Academic Editor: Yasir Nawaz

Keywords: Ionizing Oxygenated Radiotherapy Saturation effects Mathematical model

Timeline:

Received: August 11, 2025 Accepted: October 04, 2025 Published: October 19, 2025

Citation: Vithanage GVRK, Wattetenne ARMHP, Jayakody KAND, Dhanushika MS, Dassanayaka S. A mathematical model for the saturation effects of radiotherapy with oscillating tumor density. J Adv Appl Computat Math. 2025; 12: 107-120.

DOI: https://doi.org/10.15377/2409-5761.2025.12.8

**ABSTRACT** 

In the present-day society, cancer has become a challenge that threatens millions of human lives and causes many deaths. Throughout this research, we have developed a mathematical model to describe the radiotherapy treatment. There is a competition between tumor cells and normal cells; we use Lotka-Volterra dynamics to represent that biological idea in a mathematical model. In radiotherapy, ionizing particles attack the DNA of both tumor cells and normal cells. This process occurs in a medium with oxygenated tissues, and it has a saturation level. Previous researchers have not considered the saturation effects of radiotherapy in their models; however, our model incorporates the Michaelis-Menten term to represent these effects, which is the main novelty in this research with respect to previous works. We assume that other reactions are occurring according to the Mass Action Law, and also that radiotherapy targets both tumor cells and normal cells with the same intensity. First, we conduct a stability analysis of the system and then simulate the system by using time series analysis. We observed that in most cases, a stable equilibrium point can occur or periodic behavior may emerge in the population levels. By conducting a local sensitivity analysis, we identified the most sensitive parameters important in clinical treatments. We then conduct a bifurcation analysis for the most sensitive parameters, observing critical values for these parameters that must be maintained within a specific range to achieve an optimal treatment outcome. Primarily, we investigated the optimal range for the killing rate of tumor cells and discussed how the half-saturation constant effects therapy. These results will be crucial for achieving better clinical outcomes in radiotherapy.

<sup>&</sup>lt;sup>1</sup>Department of Mathematical Sciences, Wayamba University of Sri Lanka, Lional Jayathilaka Mawatha, Kuliyapitiya, 60200, Sri Lanka

<sup>&</sup>lt;sup>2</sup>Department of Mathematics and Computer Science, Wittenberg University, 200 W Ward St, Springfield, OH, 45504, USA

<sup>\*</sup>Corresponding Author Email: rohanav@wyb.ac.lk Tel: +(94) 772344312

#### 1. Introduction

Cancer is one of the most pressing public health challenges we face, accounting for millions of deaths each year. Treatment strategies like radiotherapy and chemotherapy play an imperative role in combating this disease. Meanwhile, radiotherapy is based on the use of ionizing radiation, which damages DNA irreparably in malignant cells, whereas chemotherapy is achieved through cytotoxic agents that target vital processes in growing tumor cells [1,2]. While effective, such therapies pose their unique challenges, including side effects [3, 4], tumor resistance, and personalized treatment plans [5].

Mathematical formulations provide a solid foundation for analyzing and improving cancer treatment paradigms. These types of models provide researchers with the ability to simulate the dynamics of cancer cell growth and response to therapies, while also offering insights into the interactions between cancer cells, healthy tissue, and treatment modalities [6]. Mathematical frameworks have been developed to study tumor-immune interactions and the impact of the tumor microenvironment on therapeutic outcomes, specifically for radiotherapy [7]. These models enable the evaluation of separate radiation doses and treatment schedules [8].

In chemotherapy, mathematical models based on drug pharmacokinetics and pharmacodynamics have explained the interactions between chemotherapy agents and tumor development as well as the response of the immune system [9, 10]. Such models aim to establish an optimal treatment protocol that considers the synergy and antagonism between the two modalities [11]. When comparing the side effects, chemotherapy has more side effects than radiotherapy.

This research presents a comprehensive mathematical model that analyzes the interaction between radiotherapies administered during cancer treatment. This model utilizes all the main parameters, including cancerous and healthy cell concentrations, competition coefficients, and therapy dosages. It aims to predict tumor response and guide clinicians in treatment decisions [12]. Given the complexity of tumor-therapy interactions, this research aims to develop personalized therapy strategies to achieve better clinical outcomes and minimize toxicities [13, 14]. Previous researchers in radiotherapy have not considered the saturation effects of radiotherapy in their models; however, our model takes these effects into account.

#### 2. The Model

The Lotka-Volterra model is one of the fundamental models primarily used in mathematical biology [15]. It was originally developed to model such interactions as predator-prey and competitive species in ecosystems. The phenomena expressed in coupled differential equations show how two populations affect each other through competition, predation, or mutualism [16]. The equations for competitive species take into account intrinsic growth rates, carrying capacities due to environmental factors, and competition coefficients. These parameters are crucial in illustrating how one population inhibits the growth of the other. This concept has found a wide range of applications [17], including in cancer modeling, where normal cells and cancer cells represent two competing populations within a single biological environment [18-20].

We take as our model of competition between normal and cancer cells using the idea of Lotka-Volterra dynamics with control on the cancer cells of the following system. Let  $x_1(t)$  be the density of normal cells and let  $x_2(t)$  be the density of cancer cells, then our model takes the form

$$\dot{x_1} = a_1 x_1 - b_1 x_1 x_2 - \frac{\eta x_1}{k + x_1} 
\dot{x_2} = a_2 x_2 - b_2 x_1 x_2 - \frac{\eta x_2}{k + x_2}$$
(01)

The first equation states the rate of change in density of normal cells with increasing time due to growth rate. Healthy cells grow at a rate  $a_1$  and the competition coefficient of healthy cells is represented by  $b_1$  [21-23] (Table 1). In Radiotherapy, particle beams attack the DNA's of both tumor cells and normal cells [24]. Most scientists use mass action law to interpret the attack particle beams to cells but when the radiotherapy is given there is an oxygenation

within tissues and these phenomena can enhance the effectiveness of the radiotherapy but this oxygenation process has a saturation level [24, 25]. To represent this process clearly, here we introduced a new idea that is when radiotherapy is given it has a saturation level, that part is represented by Michaelis-Menten term  $\frac{\eta x_1}{k+x_1}$  [22, 26]. This is the distruction of normal cells due to radio therapy. Here  $\eta$  is the maximum killing rate and k is the half saturation constant. According to above model the destruction of normal cells due to radiotherapy arrives at a saturation level. Here we assume radiotherapy effects on normal cells and tumor cells in the same strength. The second equation states the rate of change of density of cancer cells with time. Cancer cells grow at a rate  $a_2$ , with the competition coefficient of tumor cells, is given by  $b_2$  [9]. The term  $\frac{\eta x_2}{k+x_2}$  [27] represents the effects of radiotherapy on cancer cells, respectively.

Table1: Parameter values and sources for the model.

Parameter	Definition	Value	Ref.
$a_1$	Growth rate of healthy cells	0.1- 0.5 day <sup>-1</sup>	[21]
$a_2$	Growth rate of cancer cells	$0.45 - 0.5 \ day^{-1}$	[21]
$b_1$	Competition coefficient of healthy cells	$0.11-0.5 \ cells^{-1} \ day^{-1}$	[21]
$b_2$	Competition coefficient of cancer cells	$0.05 \text{-} 0.55 \text{ cells}^{-1} \text{ day}^{-1}$	[21]
η	Killing rate of tumor cells by radiotherapy	0.2-1.7 <i>cell</i>	[28]
k	Half Saturation constant	$0.30 - 0.75 day^{-1}$	[21]

**Theorem 1.** (i) Nonnegative quadrant of  $\mathbb{R}^2_+$  is invariant for system (01). (ii) System (01) is bounded above.

## 3. Stability Analysis of the System

Radio therapy is a novel method that uses to treat for the cancer in the modern medical treatments for tumors. In this section we are considering the treatments of radiotherapy.

$$\dot{x_1} = a_1 x_1 - b_1 x_1 x_2 - \frac{\eta x_1}{k + x_1} 
\dot{x_2} = a_2 x_2 - b_2 x_1 x_2 - \frac{\eta x_2}{k + x_2}$$
(1)

First, we need to consider the existence of the periodic orbits of this subsystem. Then it uses Dulac Criteria [26, 29, 30]. Consider  $B(x_1, x_2) = \frac{1}{x_1 x_2}$  and it is continuously differentiable on  $\mathbb{R}^2_+$ .

$$\begin{split} f_1 &= a_1 x_1 - b_1 x_1 x_2 - \frac{\eta x_1}{k + x_1} \\ f_2 &= a_2 x_2 - b_2 x_1 x_2 - \frac{\eta x_2}{k + x_2} \\ \frac{\partial B f_1}{\partial x_1} + \frac{\partial B f_2}{\partial x_2} &= \eta \left[ \frac{1}{x_2 (k + x_1)^2} \right] + \eta \left[ \frac{1}{x_1 (k + x_2)^2} \right] \end{split}$$

According to Dulac Criteria if  $\frac{\partial Bf_1}{\partial x_1} + \frac{\partial Bf_2}{\partial x_2} > 0 \ \forall x_1, x_2$  in first quadrant. It has positive sign, then there are no positive periodic orbits in the first quadrant.

Proposition 1: System (01) hasn't any positive periodic solutions in  $\mathbb{R}^2_+$ .

We proceed to discuss the existence of positive equilibria for the subsystem (2). From direct calculations we can obtain 3 equilibrium points rapidly. They are (0,0),  $(0,\frac{\eta}{a_2}-k)$  and  $(\frac{\eta}{a_1}-k,0)$ . Here we are assigning a condition to

make none zero components as positive values otherwise they are not meaningful. We need to set the parameters as  $\frac{\eta}{a_2} > k$  and  $\frac{\eta}{a_1} > k$ . Third equilibrium point is biologically important as normal cell density is becoming zero is an unusual phenomenon. Then we are going to consider about the positive equilibrium points by considering the geometry of non-trivial  $x_1$  and  $x_2$  ioclines.

$$f(x_1) = x_2 = \frac{a_1}{b_1} - \frac{\eta}{b_1(k+x_1)}$$

$$g(x_1) = x_2 = \frac{\eta}{a_2 - b_2 x_1} - k$$

Here  $f'(x_1) > 0$  in  $\mathbb{R}^2_+$  and  $\lim_{x_1 \to 0^+} f(x_1) = \frac{a_1}{b_1} - \frac{\eta}{b_1 k} < 0$  and then f intersects x axis at  $(\frac{\eta}{a_1} - k, 0)$  and finally f arrives to a steady level  $\lim_{x_1 \to \infty} f(x_1) = \frac{a_1}{b_1} > 0$ .  $g(0) = \frac{\eta}{a_2} - k$  and here  $g'(x_1) > 0$  in  $[0, \frac{a_2}{b_2})$  and then  $\lim_{x_1 \to \frac{a_1}{b_1}} g(x_1) \to \infty$  also  $\lim_{x_1 \to \frac{a_1}{b_1}} g(x_1) \to -\infty$  and  $\lim_{x_1 \to \infty} g(x_1) \to -k$ . g > 0 in  $[0, \frac{a_2}{b_2})$  then g < 0 in  $(\frac{a_2}{b_2}, \infty)$ . If these 2 curves intersect, we only consider the first quadrant. Mainly it

 $\lim_{x_1 \to \infty} g(x_1) \to -k$ . g > 0 in  $[0, \frac{\omega_2}{b_2})$  then g < 0 in  $(\frac{\omega_2}{b_2}, \infty)$ . If these 2 curves intersect, we only consider the first quadrant. Mainly it can occur 3 cases for the existence of positive equilibrium points. Consider 3 cases (Fig. (1). If these 2 curves do not intersect there is not any positive equilibrium point. If these 2 curves touch each other it can occur only one positive equilibrium point. If these 2 curves intersect it can occur 2 positive equilibrium points. From below diagrams we can observe that how there exist positive equilibrium points according to the intersection of non-trivial isoclines. Here red color represents g curve and green represent f curve.

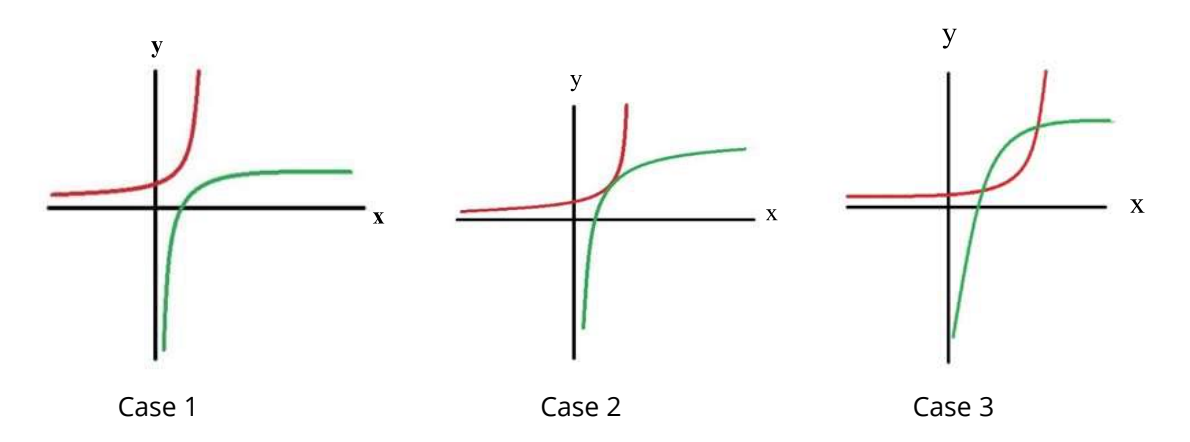


**Figure 1:** Geometrical behavior of non-trivial isoclines in xy – plane.

We have obtained that  $\lim_{x_1 \to \infty} f(x_1) = \frac{a_1}{b_1} > 0$  and  $g(0) = \frac{\eta}{a_2} - k$ . Then we can have that, if  $\frac{\eta}{a_2} - k > \frac{a_1}{b_1}$  then there are no any positive equilibrium points for this subsystem. If  $\frac{\eta}{a_2} - k < \frac{a_1}{b_1}$  then it can occur no positive equilibrium points or at most 2 positive equilibrium points for this subsystem. Next, we move to consider the stability of all these equilibrium points.

We are going to use Jacobian to discuss the stability of equilibrium points and their asymptotic dynamics.

$$J = \begin{bmatrix} a_1 - b_1 x_2 - \frac{\eta k}{(k+x_1)^2} & -b_1 x_1 \\ -b_2 x_2 & a_2 - b_2 x_1 - \frac{\eta k}{(k+x_2)^2} \end{bmatrix}$$
(3)

First let's consider (0,0) equilibrium point.

$$J(0,0) = \begin{bmatrix} a_1 - \frac{\eta}{k} & 0\\ 0 & a_2 - \frac{\eta}{k} \end{bmatrix}$$

It shows that the real parts of both eigen values are negative and there is a stable node. It implies that (0,0) steady state is locally asymptotically stable. Consider about the equilibrium point  $\left(0,\frac{\eta}{a_2}-k\right)$ . After applying this equilibrium point to the Jacobian, we can observe that if the trace becomes negative then tumor density component becomes negative hence, we can obtain this equilibrium point is not a stable equilibrium point. Consider the equilibrium point  $\left(\frac{\eta}{a_1}-k,0\right)$ . This steady state is biologically important. If this equilibrium point becomes stable means we can remove the cancer completely by radiotherapy. After applying this equilibrium point to the Jacobian, we can observe that if the trace becomes negative then the normal cell density component becomes negative hence, we can obtain this steady state is not a stable point. If there is at least one positive equilibrium or at most two positive equilibrium points it needs to be considered about their stability. Take that equilibrium point as  $(x_1^*, x_2^*)$  and it can obtain the trace of the Jacobian as  $\left[\frac{x_1^*}{(k+x_1)^2} + \frac{x_2^*}{(k+x_2)^2}\right] > 0$ . This implies at least one eigen value is positive hence it gives if there exist one or two positive equilibrium points, they become unstable. Biologically it supplies an important result, that is by using radiotherapy under the saturation effects we can't stabilize the tumor and normal cells at a fixed level. On the other hand, it is difficult to remove tumor completely while keeping normal cells at a constant level.

**Theorem 2:** In the region  $R_x = \{(x_1, x_2) \in \mathbb{R}^2_+: x_1 > 0, x_2 > 0\}$  the equilibrium point (0,0) is locally asymptotically stable. The equilibrium points  $\left(0, \frac{\eta}{a_2} - k\right)$  and  $\left(\frac{\eta}{a_1} - k, 0\right)$  and other positive equilibrium points are not stable.

Mainly in radiotherapy it ionizes the DNA of cancer cells or the therapy can shrink the tumor, but sometimes it can harm normal cells [31, 32]. If it gives a high dose, it can harm both tumor and normal cells [24], there we can see that our system (0,0) becomes locally asymptotically stable in such a situation. In next section we focus on numerical simulations of the system.

## 4. Numerical Simulations of the System

In this section, we utilize numerical simulations to gain insight into the interactions between tumors and radiotherapy. Here we use MATLAB software for our simulations. Here, we utilized the ODE 45 package [33] in discrete time intervals, employing the Runge-Kutta Method [34, 35] to obtain the figures in this section. When it is given radiotherapy, it can kill cells; on the other hand, these beams can slow the growth by damaging their DNA, and these cells are destroyed gradually. On the other hand, radiotherapy harms normal cells [21]. The blue line represents normal cell density, and the green line represents tumor cell density. k is the half-saturation constant of the radiotherapy effect. Here we are giving the therapy every 2 days. We are supposed to give the treatment for 20 days. Initially, radiotherapy is also administered.

We have taken initial conditions as  $x_{10} = 0.8$  and  $x_{20} = 0.425$ . Fig. (2) for all the diagrams  $\eta = 0.3$ . Fig. (2), in first graph  $a_1 = 0.49$ ,  $a_2 = 0.49$ , k = 0.6 in second graph  $a_1 = 0.35$ ,  $a_2 = 0.35$ , k = 0.8, in third graph  $a_1 = 0.29$ ,  $a_2 = 0.29$ , k = 1.0005. Here k plays a crucial role, when k = 0.6 both normal cell density and tumor cell density are drastically decreasing. There we can observe that with the first couple of weeks both cell densities decreasing rapidly but in the last week of the treatment decreasing rate becomes small. When k = 0.8 normal cells decrease but it's not like in first graph in Fig. (2) tumor cells are also decreasing and it's very important that at the first week of the treatment tumor level decreasing strongly and for the other two weeks tumor level decrease in a constant way, but that decrement rate is slight. We can observe that it is decreasing from 4.25 to 2.5. When k = 1.0005 we can observe that, although we give radiotherapy normal cell density is always approach to a constant level but tumor density gradually decreasing, this is very effective at it doesn't make too much harm for normal cells. It gives an impressive result that if we can keep k near 1 or slightly greater than 1 we can reduce tumor density while keeping normal cell density at a fixed level. When we consider about saturation effects, if we can keep saturation constant level near 1, we can get effective results to reduce tumor. But we need to fix other parameters appropriately for k.

Then let us focus on the killing rate of tumor cells by radiotherapy. According to this model, when radiotherapy is given, both normal cells and tumor cells are killed. The blue line represents normal cell density, and the green line

represents tumor cell density. Here, we administer the therapy every 2 days. We are supposed to give the treatment for 20 days. Initially, radiotherapy is also given on the scheduled date.

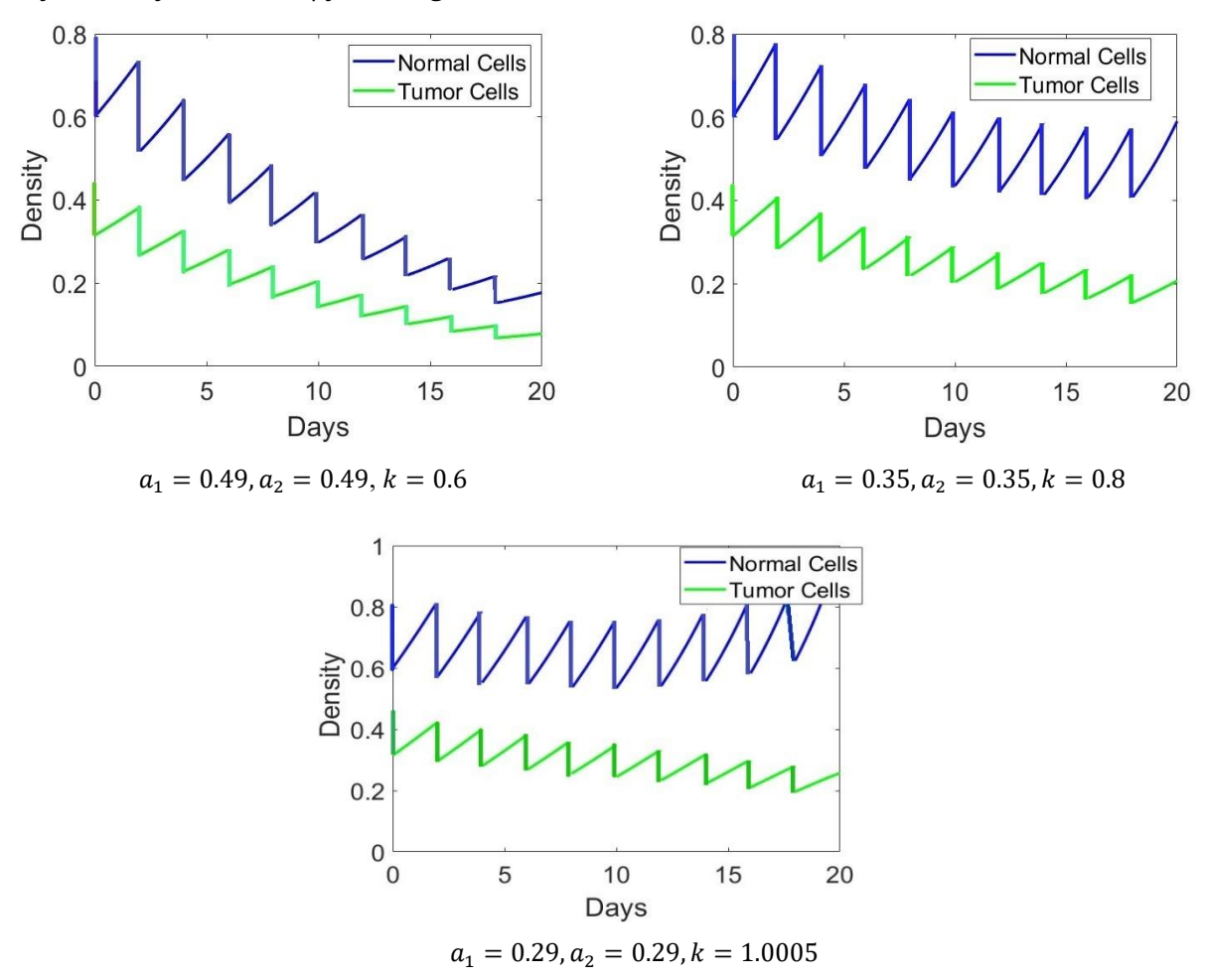


**Figure 2:** Time series analysis for the tumor density and normal cell density for different half saturation constants.

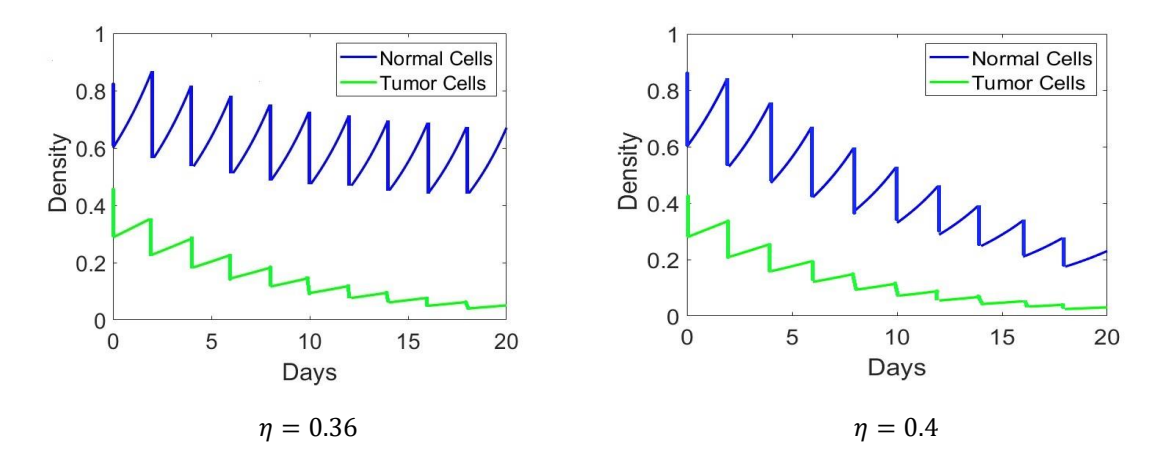


Figure 3: Time series analysis for the tumor density and normal cell density for different killing rate tumor cells by radiotherapy.

We have taken initial conditions as  $x_{10} = 0.83$  and  $x_{20} = 0.48$ . Here we have set the parameters as  $a_1 = 0.46$ ,  $b_1 = 0.2$ ,  $a_2 = 0.46$ ,  $b_2 = 0.2$ , k = 1.0005. In Fig. (3) first diagram we choose  $\eta = 0.36$  there we can observe in the first week tumor density is decreasing drastically then radiotherapy is given continuously and in the second week also tumor density is decreasing but decrement is not like in the first week. In the treatment of the third week, we can observe that tumor population decreasing little by little for each therapy time and the important thing is this we can observe

this radiotherapy harm to normal cells but after 3 weeks decrement is a slight amount with respect to the decrement of the tumor density. Ionizing radiation can damage DNA and regulatory of proteins [36]. This is a disadvantage in radiotherapy. Then let's increase killing rate of tumor cells by radiotherapy by a slight amount as  $\eta=0.4$  in Fig. (3) second graph. We can see that with a slight increment of  $\eta$  it can become considerable harm for normal cells. At the beginning Normal cell density is 0.83 then uniformly that density has approached to 0.21, it seems even a slight increment of the  $\eta$  can make a big harm for the treated area, so it is needed to be careful. The biological target of radiation in the cell is DNA.

DNA double-strand breaks can cause more killing of cells than single-strand breaks [37]. Mainly due to these breaks, it can disrupt its genomic integrity [38] through radiotherapy [25, 31, 39]. Cancer cells are surrounded by normal cells, so in a radiotherapy treatment, a high-energy particle of radiation can harm both normal cells and tumor cells [25, 36, 40]. By using radiotherapy, it is necessary to kill tumor cells, but on the other hand, it is also necessary to be careful about the harm it causes to normal cells. Due to the lack of data and complexity of the model, we assume that the impact of radiotherapy on normal cells and tumor cells is the same. If radiotherapy primarily affects cancer cells, tumor density will decrease rapidly, and the rate of tumor cell decrement may be greater than that of normal cells. In that treatment, harm to normal cells is less than in our model, making it a more successful treatment method in radiotherapy. In the next section, we focus on how each parameter affects the final tumor density through sensitivity analysis.

## 5. Model Outcomes and Sensitivity Analysis

To deepen our understanding of parameter influence on tumor dynamics, we performed a local sensitivity analysis [41, 42] of key model parameters by perturbing each parameter [43, 44] by  $\pm 10\%$  from its baseline and evaluating the relative change [45, 46] in final tumor density  $(x_2)$ . The results are summarized in Tables **2** and **3** and the original values are taken from the Table **1**.

Table 2: Parameter sensitivity analysis: effect on final tumor density ( $x_2$ ).

Parameter	Variation	Parameter Value	x <sub>2</sub> Change (%)
$a_1$	Base	0.46	0.0
$a_1$	+10%	0.506	-39.7
$a_1$	-10%	0.414	-100.09
$a_2$	Base	0.46	0.0
$a_2$	+10%	0.506	-93.25
$a_2$	-10%	0.414	-101.07
$b_1$	Base	0.2	0.0
$b_1$	+10%	0.22	-54.13
$b_1$	-10%	0.18	-98.85
$b_2$	Base	0.2	0.0
$b_2$	+10%	0.22	-24.45
$b_2$	-10%	0.18	-101.09
k	Base	1.0	0.0
k	+10%	1.101	-105.36
k	-10%	0.9	-101.71
η	Base	0.36	0.0
η	+10%	0.396	-101.26
η	-10%	0.324	-97.39

Table **2** evaluates how sensitive the final tumor density  $(x_2)$  is to variations in parameters including:  $a_1$ ,  $a_2$  (growth rates),  $b_1$ ,  $b_2$  (competition coefficients), k (killing rate by radiotherapy), and  $\eta$  (radiotherapy dose). Changes in k and  $\eta$  resulted in over 100% variation in  $x_2$ , indicating extreme sensitivity. For example, a 10% increase in k led to a 105.36% reduction in tumor density, while a 10% increase in  $\eta$  caused a 101.26% reduction. Furthermore, Similar high impacts were seen for  $a_2$  and  $a_2$ , indicating their strong roles in tumor dynamics.

Table 3: Parameter sensitivity ranking (Ordered by impact on final  $x_2$ ).

Parameter	+10% Effect (%)	-10% Effect (%)	Avg Absolute Effect (%)	Max Effect (%)
k	-105.36	-101.71	103.53	105.36
η	-101.26	-97.39	99.33	101.26
$b_2$	-24.45	-101.09	62.77	101.09
$a_2$	-93.25	-101.07	97.16	101.07
$a_1$	-39.7	-100.09	69.89	100.09
$b_1$	-54.13	-98.85	76.49	98.85

Table **3** ranks the parameters by average and maximum effect. The top three most sensitive parameters are  $k, \eta$ , and  $b_2$ . These findings suggest that precise calibration of radiotherapy-related parameters is essential for successful tumor control. Even small variations in these parameters significantly affect the outcome, reinforcing the need for precision-based treatment protocols. A graphical representation of this summary can be seen in the Appendix **A** section.

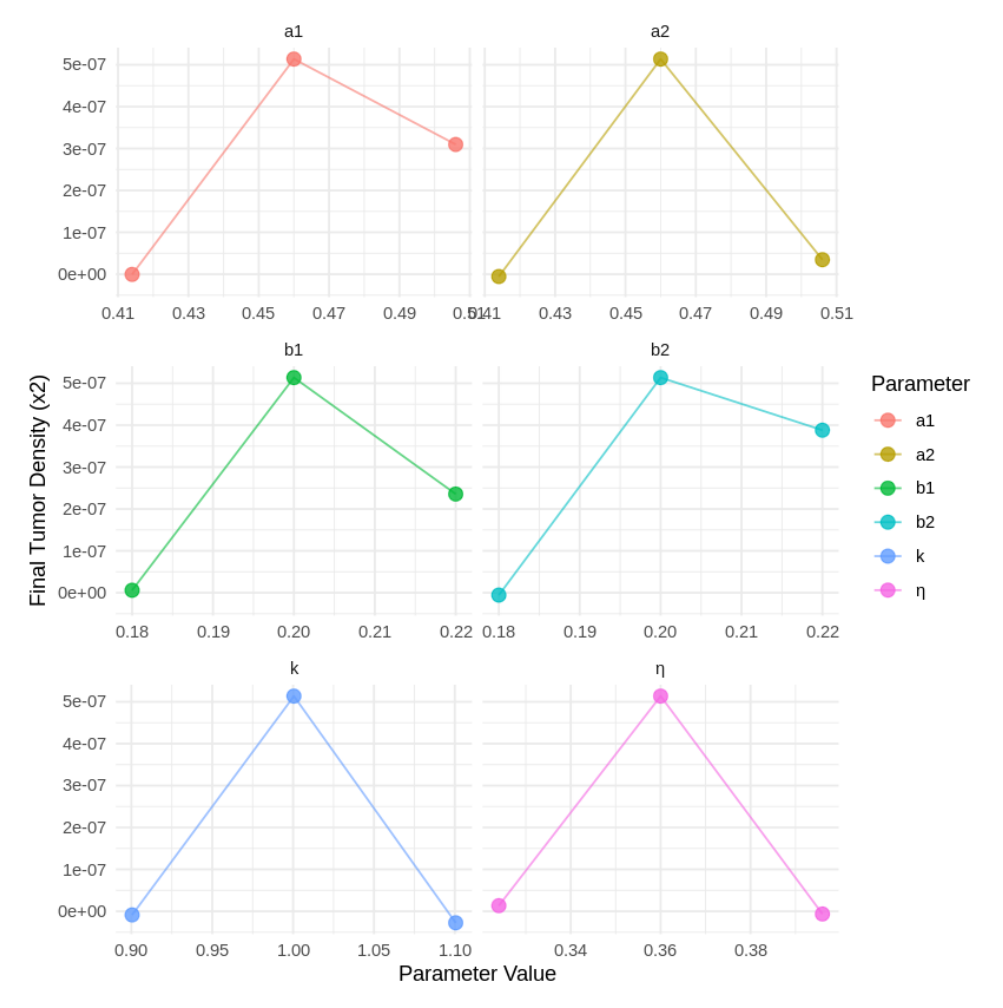


Figure 4: Parameter value vs final tumor density.

On the other hand, we monitored the final tumor density changes with the most sensitive parameters and Fig. (4) describes it graphically. This figure illustrates how the final tumor density changes as a function of each model parameter, particularly those identified as most sensitive according to Table 3. The x-axis shows the perturbed values of a parameter and here it increased or decreased ±10% from the baseline. The y-axis shows the corresponding final tumor cell density after the 20-day treatment period. The plot illustrates how even a slight change in specific parameters can significantly reduce tumor density, or conversely, render treatment ineffective. Higher sensitivity implies a narrow therapeutic window; a slight miscalibration could lead to either ineffective treatment or excessive damage to normal cells. This figure supports the idea that precision in dosing is crucial in optimizing cancer treatment outcomes.

Moreover, the final tumor density can be analyzed for a 20-day time stamp with the top three most sensitive parameters in Fig. (5). This figure displays time-course simulations of tumor density under perturbations of the three most sensitive parameters, facilitating visualization of how tumor suppression evolves over the 20-day treatment period. The x-axis represents time in days from 0 to 20, while the y-axis represents tumor cell density. Multiple curves correspond to different parameter settings. When sensitive parameters are increased, tumor density drops rapidly and stabilizes near zero, sometimes achieving eradication. Decreasing these same parameters by 10% results in a much slower decay or even persistence of the tumor, indicating suboptimal therapy. Further, this illustrates the critical importance of maintaining adequate parameter levels, especially for k,  $a_2$ , and  $\eta$ .

In Fig. (6) shows how the number of cancer cells changes over a 21-day treatment period, with different levels of radiotherapy doses ( $\eta$ ). Each colored line indicates a simulation at a specific dose, from 0.1 to 0.5. Initially, the cancer cell counts increases and reaches its peak within the first 4 to 5 days. After that, the number drops quickly, with the population nearing zero around day 8 and staying low through day 21. While all doses exhibit a similar overall pattern, higher  $\eta$  levels (such as 0.5, shown in yellow) tend to accelerate the decline and slightly lower the peak compared to lower doses (such as 0.1, shown in dark blue). This suggests that stronger radiotherapy can more effectively suppress the tumor, although the differences between doses become less noticeable once the cell population drops considerably. Overall, the results show that the treatment is quite effective across different radiation levels, with all doses eventually leading to the disappearance of cancer cells under the conditions modeled.

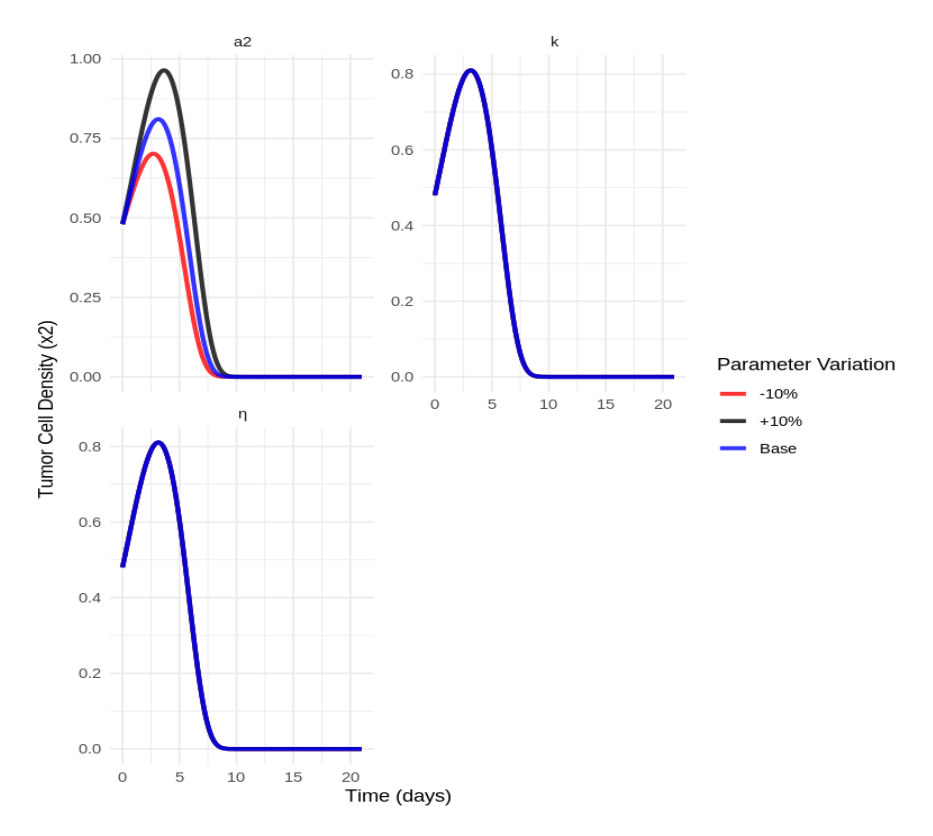
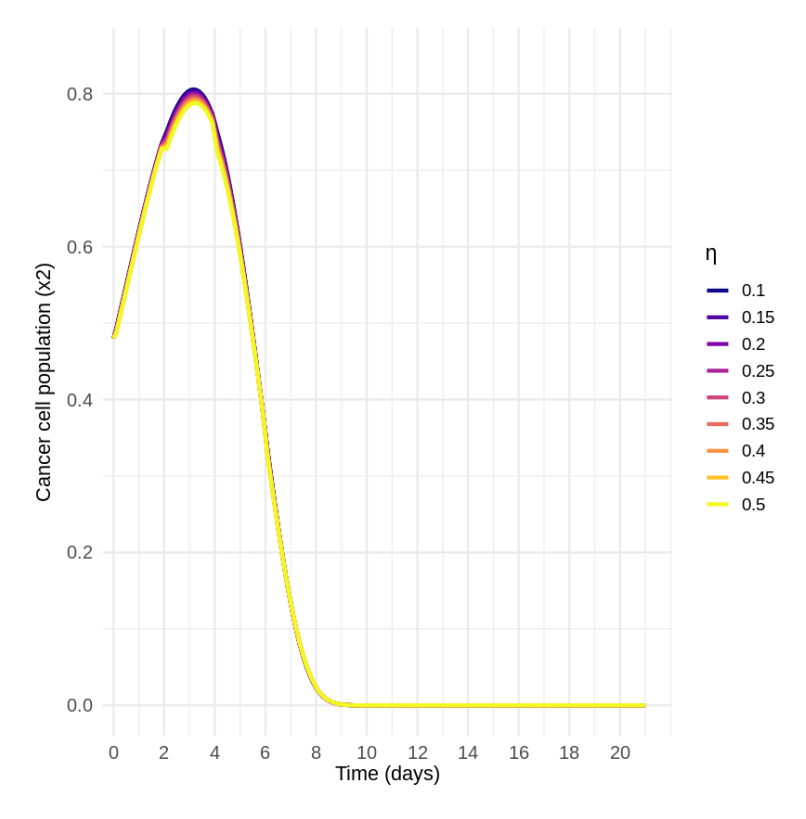


Figure 5: Tumor density for most sensitive parameters.

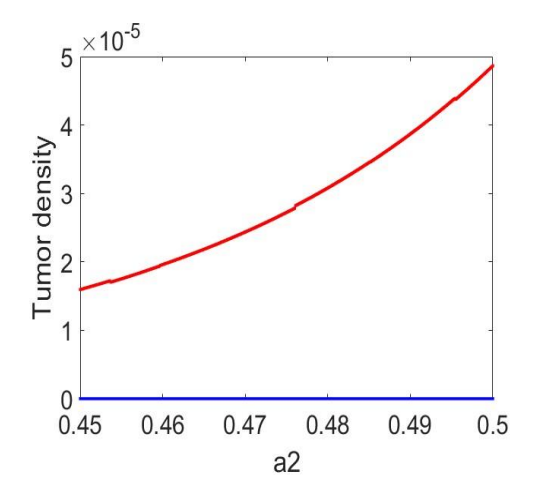


**Figure 6:** Cancer cell population (x2) over time for different radiotherapy doses.

From a clinical perspective, the model emphasizes optimizing radiotherapy dosage and enhancing tumor radiosensitivity. The narrow tolerance window of these parameters underscores the importance of patient-specific calibration, supporting the case for personalized radiotherapy strategies. In next section we are conducting a bifurcation analysis for the most sensitive parameters.

## 6. Bifurcation Analysis for the Most Sensitive Parameters

In this section we suppose to conduct a bifurcation analysis [26, 45] for the parameters  $a_2$ , k and  $\eta$ . Here  $a_2$  plays a critical role as it is the growth rate of tumor cells. In this context, we are using MATLAB for the simulations, and we are taking the initial conditions as  $x_{10}=0.65$  and  $x_{20}=0.25$ . We keep other parameters as in Table 2 and change  $a_2$  from 0.45 to 0.5.



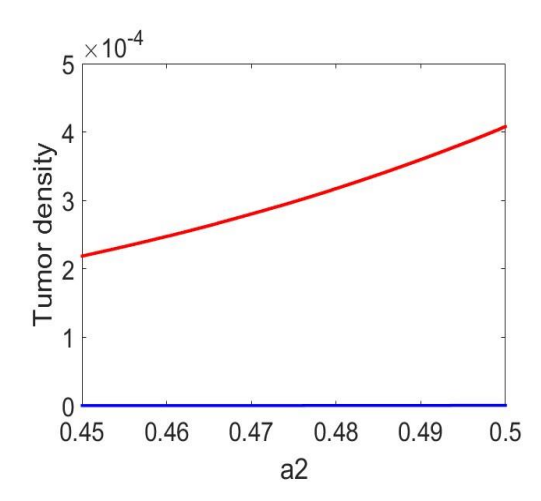


Figure 7: bifurcation diagram for growth rate of tumor cells.

In this diagram, red color represents the maximum value of tumor density, and blue color represents the minimum value of tumor density. In Fig. (7), the first diagram gives a weak radiotherapy dose,  $\eta=0.36$  and in Fig. (7), the second diagram gives a strong radiotherapy dose  $\eta=0.66$ . It can be observed that the tumor density oscillates when the growth rate of tumor cells increases. Here, an interesting phenomenon happens: on one side, tumor cells are growing, and on the other hand, radiotherapy attacks the DNA [25, 39] of these tumor cells. Then, tumor density decreases; however, it increases again when no radiotherapy treatment is given. As it occurs, this cycle pattern during the treatment time generates oscillations for tumor density, and it can decrease or increase according to the initial conditions and other parameter values, as described in Fig. (2) and Fig. (3). Then, let's consider the  $\eta$ , the killing rate of tumor cells by radiotherapy. The intensity of the radiotherapy is also an important factor in cancer treatment. Here we keep  $\chi_{10}=0.65$  and  $\chi_{20}=0.25$  and change  $\eta$  from 0.4 to 0.7 also other parameter values are taken from Table 2.

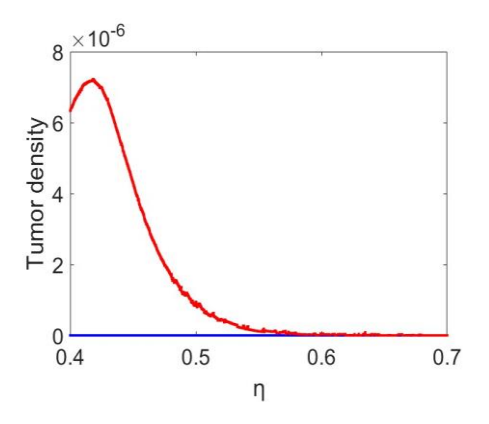


Figure 8: bifurcation diagram for killing rate of tumor cells by radiotherapy.

Here (Fig. **8**), a Hopf bifurcation occurs when  $\eta$  arrives at 0.585. When  $\eta$  is in [0.4,0.585) tumor density is oscillating, as in Fig. (**2**) and Fig. (**3**), but when the killing rate of the tumor cells by radiotherapy is increasing, that cyclic pattern changes to (0,0) equilibrium point, as we can observe in (0.585,0.7] maximum and minimum of tumor densities overlap on each other, and in that case, the tumor density is in 0 level. This reveals a result that, at a strong rate of  $\eta$ , it can severely harm normal cells; in clinical treatment, it is necessary to be cautious about the limitations of the killing rate of tumor cells by radiotherapy. The half-saturation constant also plays a crucial role in this radiotherapy treatment. We take the initial condition as  $x_{10} = 0.60$  and  $x_{20} = 0.25$  and we keep other parameters as in Table **2** and change k from 0 to 2.

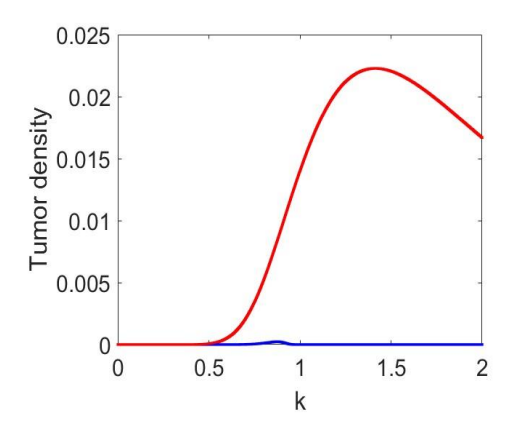


Figure 9: Bifurcation diagram for half saturation constant.

It can observe that when  $k \in [0.2,0.5)$ , it occurs a steady state with zero tumor density, then tumor level oscillates and when k = 1.4 this difference between maximum tumor level and minimum tumor level becomes maximum. In Fig. (2) second diagram k = 0.6 there we observed that both tumor level and normal cell density level arrives to (0,0) equilibrium drastically, in Fig. (2), the second diagram, k = 0.8 and both levels oscillates and in Fig. (2) third diagram

k=1.0005, there difference between maximum and minimum levels increase. This illustrates that when the half saturation is in a small value radiotherapy becomes harmful for normal cells severely. It needs to keep half saturation level to an optimal level to keep the therapy success.

#### 7. Conclusion

Radiotherapy is like a double-edged sword, as on one hand, radiation waves generate particle beams and they can harm the DNA of both cancer cells and tumor cells [25, 24, 47]. We developed a model using Lotka-Volterra dynamics and saturation effects for radiotherapy treatment [16, 19, 20]. In the stability analysis of the equilibrium points, we found that the origin is the only possible stable equilibrium point under certain parameter conditions. The model exhibits a complex dynamical behavior, where tumor density and normal cell density oscillate in a pattern during the treatment period. Additionally, one population density cannot approach zero, while the other population remains at a steady level.

Then, we conducted a local sensitivity analysis [41, 42] to observe the model outcomes, primarily seeking to identify the most essential parameters that can affect the final tumor density. We observed that the growth rate of cancer cells, the killing rate of tumor cells by radiotherapy, and the half-saturation constant have a considerable effect on the final tumor density and the treatment outcome. When deciding on a radiotherapy treatment, the size of the tumor, the stage of the cancer, and its location in the body are important factors to consider. Throughout this research, we investigate the growth rate of cancer cells, the effectiveness of radiotherapy, and the saturation level, all of which are important factors in deciding on a radiotherapy treatment. This finding will be important in clinical treatments.

Finally, we conducted a bifurcation analysis [48, 49] for the most sensitive parameters individually to observe their behavior and how the asymptotical dynamics of the system change according to their behavior. When  $\eta$  is increasing, we observed that the periodic behavior of the treatment changed to a steady level, resulting in both population densities reaching zero. This reveals that high intensities of the radiotherapy treatment do not yield successful results, as they also have harmful effects on normal cell density. Here, we identified threshold levels for  $\eta$  from our numerical simulations of the Hopf bifurcation [49, 47]. When considering the saturation level, k, we observed that it needs to be kept at an optimal value to get an optimal clinical outcome [50]. Fig. (9), we can see that a minimal value of k, therapy is not successful. It needs to control these parameters with good precision, as we know radiation can have a significant effect on not only cancer but also on normal cells; hence, they need to manipulate radiotherapy within a suitable parameter range, otherwise therapy can be harmful to the patient. We hope these results will help improve cancer treatment methods in radiotherapy for the future.

#### **Conflict of Interest**

The authors declare that there is no conflict interest.

## **Funding**

This work is not supported by any external funding.

## **Acknowledgments**

Gratitude is extended to our research team and Dr. Sachith Dassanayaka for his contribution to this project through his sensitivity analysis. Ms. M.S. Dhanushika, Ms. Nirupadi Diwyani, and Ms. Hasini Parami Wattetenne for their analysis and support in data collection and numerical analysis. We also extend our gratitude to Dr. Sophia Jang from Texas Tech University for her support.

#### References

[1] Hall EJ, Giaccia AJ. Radiobiology for the radiologist. Philadelphia: Lippincott Williams & Wilkins; 2012.

- [2] Chabner BA, Longo DL. Cancer chemotherapy and biotherapy: principles and practice. Philadelphia: Lippincott Williams & Wilkins; 2011.
- [3] Kaur S, Mayanglabam P, Bajwan D. Chemotherapy and its adverse effects. Int J Nurs Edu Res. 2022; 10(2): 113-7. https://doi.org/10.52711/2454-2660.2022.00090
- [4] Altun I, Şenkaya A. The most common side effects experienced by patients receiving first cycle of chemotherapy. Iran J Public Health. 2018: 47(8): 1128-35.
- [5] Hanahan D, Weinberg RA. Hallmarks of cancer: the next generation. Cell. 2011; 144(5): 646-74. https://doi.org/10.1016/j.cell.2011.02.013
- [6] De Pillis LG, Radunskaya AE, Wiseman CL. A validated mathematical model of cell-mediated immune response to tumor growth. Cancer Res. 2005; 65(17): 7950-8. https://doi.org/10.1158/0008-5472.CAN-05-0564
- [7] Powathil GG, Gordon KE, Hill LA, Chaplain MAJ. Modelling the effects of cell-cycle heterogeneity on the response of a solid tumour to chemotherapy. Math Biosci. 2013; 245(2): 162-73.
- [8] Bertuzzi A, Fasano A, Gandolfi A. A mathematical model for tumor growth: analysis of the role of vascularization. Math Models Methods Appl Sci. 2003; 13(11): 1731-49.
- [9] Panetta JC. A mathematical model of drug resistance: heterogeneous tumors. Math Biosci. 1997; 147(1): 41-61. https://doi.org/10.1016/S0025-5564(97)00080-1
- [10] Garay T. Competition dynamics in a tumor-immune model with chemotherapeutic treatment. Bull Math Biol. 2013; 75(9): 1460-80.
- [11] Naldi A, Carneiro J, Chaouiya C, Thieffry D. Diversity and plasticity of Th cell types predicted from regulatory network modelling. PLoS Comput Biol. 2010; 6(9): e1000912. https://doi.org/10.1371/journal.pcbi.1000912
- [12] Świerniak A, Poleszczuk J, Ochab-Marcinek A. Optimal protocols in combined anticancer therapy. Math Biosci Eng. 2009; 6(4): 739-50.
- [13] Tracqui P. Biophysical models of tumor growth. Rep Prog Phys. 2009; 72(5): 056701. https://doi.org/10.1088/0034-4885/72/5/056701
- [14] Griggs JJ. Reducing the toxicity of anticancer therapy: new strategies. Leuk Res. 1998; 22(1): 17-22. https://doi.org/10.1016/S0145-2126(98)00036-8
- [15] Crittiana M. Lotka-Volterra and their model. Didact Math. 2014; 32(2): 45-9.
- [16] Lotka AJ. Elements of physical biology. Baltimore: Williams & Wilkins; 1925.
- [17] Tahara T, Gavina MKA, Kawano T, Tubay JM, Rabajante JF, Ito H, et al. Asymptotic stability of a modified Lotka–Volterra model with small immigrations. Sci Rep. 2018; 8: 25436. https://doi.org/10.1038/s41598-018-25436-2
- [18] Muller H, Schimidit G, Ficher L. Lotka-Volterra model with principal component analysis. J Comput Biol Med. 2024; 4(4): 96-101. https://doi.org/10.71070/jcbm.v4i1.96
- [19] Murray JD. Mathematical biology I: an introduction. New York: Springer; 2002. https://doi.org/10.1007/b98868
- [20] Gatenby RA, Maini PK. Mathematical oncology: cancer summed up. Nature. 2003; 421(6921): 321. https://doi.org/10.1038/421321a
- [21] Liu Z, Yang C. A mathematical model of cancer treatment by radiotherapy. J Appl Math. 2014; 2014: 172923. https://doi.org/10.1155/2014/172923
- [22] Freedman HI. Deterministic mathematical models in population ecology. New York: Marcel Dekker; 1980.
- [23] Clotilda AMD, Vithanage GVRK, Lakshika DD. A mathematical model to treat cancer using chemotherapy and immunotherapy under mass action kinetics for immunotherapy. Math Comput Model Appl. 2024; 4: 150. https://doi.org/10.37394/232023.2024.4.15
- [24] Conocapka M, Rogolinski J, Sochanik A. Can high dose use in radiotherapy change therapeutic effectiveness? Contemp Oncol. 2017; 20(6): 449-52. https://doi.org/10.5114/wo.2016.65603
- [25] Baskar R, Lee KA, Yeo R, Yeoh KW. Cancer and radiation therapy: current advances and future directions. Int J Med Sci. 2012; 9(3): 193-9. https://doi.org/10.7150/ijms.3635
- [26] Vithanage GVRK, Wei HC, Jang SRJ. Bistability in a model of tumor–immune system with oncolytic viral therapy. Math Biosci Eng. 2022; 19(7): 2072. https://doi.org/10.3934/mbe.2022072
- [27] Lestari D, Sari ER, Arifash H. Dynamics of a mathematical model with chemotherapy. J Phys Conf Ser. 2018; 1320(1): 012026. https://doi.org/10.1088/1742-6596/1320/1/012026
- [28] Prokopiou S, Moros EG, Poleszczuk J, Caudell J, Torres-Roca JF, Latifi K, et al. A proliferation saturation index to predict radiation response and personalize radiotherapy fractionation. Radiat Oncol. 2015; 10: 145. https://doi.org/10.1186/s13014-015-0465-x
- [29] Gasull A, Giacomini H. Effectiveness of the Bendixson–Dulac theorem. J Differ Equ. 2021; 305: 283-96. https://doi.org/10.1016/j.jde.2021.10.011
- [30] McCluskey C, Muldowney J. Bendixson–Dulac criteria for difference equations. J Dyn Differ Equ. 1998; 10(4): 541-56. https://doi.org/10.1023/A:1022677008393
- [31] Azad R, Aghdam EK, Rauland A, Jia Y, Avval AH, Bozorgpour A, et al. Medical image segmentation review: the success of U-net. IEEE Trans Pattern Anal Mach Intell. 2024; 46(2): 1234-52. https://doi.org/10.1109/TPAMI.2024.3435571
- [32] Akuzinov AA, Rozhina EE, Resistance to radiotherapy in cancer. Dis. 2025; 13(1): 22. https://doi.org/10.3390/diseases13010022
- [33] Abelman S, Patidar KC. Comparison of some recent numerical methods for initial value problems for stiff ordinary differential equations. Comput Math Appl. 2008; 55(4): 1215-25. https://doi.org/10.1016/j.camwa.2007.05.012
- [34] Shampine C, Reichelt M. The MATLAB ODE suite. SIAM J Sci Comput. 2006; 18(1): 1-22.

- [35] Ashino R, Nagase M, Vaillancourt R. Behind and beyond the MATLAB ODE suite. Comput Math Appl. 2000; 40(4-5): 491-512. https://doi.org/10.1016/S0898-1221(00)00175-9
- [36] Hubenak JR, Zhang Q, Branch CD, Kronowitz SJ. Mechanisms of injury to normal tissue after radiotherapy: a review. Plast Reconstr Surg. 2014; 133(1): 49-56. https://doi.org/10.1097/01
- [37] Toulany M. Targeting DNA double-strand break repair pathways to improve radiotherapy response. Genes. 2019; 10(1): 25. https://doi.org/10.3390/genes10010025
- [38] Vignard J, Mirey G, Salles B. Ionizing-radiation induced DNA double-strand breaks: a direct and indirect lighting up. Radiother Oncol. 2013; 108(3): 362-9. https://doi.org/10.1016/j.radonc.2013.06.013
- [39] Sekhoacha M, Riet K, Motloung P, Gumenku L, Adegoke A, Mashele S. Prostate cancer review: genetics, diagnosis, treatment options, and alternative approaches. Molecules. 2022; 27(17): 5730. https://doi.org/10.3390/molecules27175730
- [40] Vithanage GVRK, Jang SRJ. Optimal immunotherapy interactions in oncolytic viral therapy and adoptive cell transfer for cancer treatment with saturation effects. WSEAS Trans Biol Biomed. 2025; 22: 23. https://doi.org/10.37394/23208.2025.22.23
- [41] Buljan I, Benkovic M. Simulation and local parametric sensitivity analysis of a computational model of fructose metabolism. Processes. 2025; 13(1): 125. https://doi.org/10.3390/pr13010125
- [42] Mester R, Landeros A, Rackauckas C. Differential methods for assessing sensitivity in biological models. PLoS Comput Biol. 2022; 18(6): e1009598. https://doi.org/10.1101/2021.11.15.468697
- [43] Lakrisenko P, Pathirana D, Weindl D, Hasenauer J. Benchmarking methods for computing local sensitivities in ordinary differential equation models at dynamic and steady states. PLoS One. 2024; 19(4): e0312148. https://doi.org/10.1371/journal.pone.0312148
- [44] Charzynska A, Nalecz A, Rybinski M, Gambin A. Sensitivity analysis of mathematical models of signaling pathways. Biotechnologia. 2012; 93(3): 245-54. https://doi.org/10.5114/bta.2012.46584
- [45] Savatorova V. Exploring parameter sensitivity analysis in mathematical modeling with ordinary differential equations. CODEE J. 2023; 16: 4. https://doi.org/10.5642/codee.CZKZ5996
- [46] Burrage K, Burrage PM, Kreikemeyer JN. Learning surrogate equations for the analysis of an agent-based cancer model. Front Appl Math Stat. 2025; 11: 1578604. https://doi.org/10.3389/fams.2025.1578604
- [47] Adi-Kusumo F, Aryati L, Risdayati S, Norhidayah S. Hopf bifurcation on a cancer therapy model by oncolytic virus involving the malignancy effect and therapeutic efficacy. Int J Math Math Sci. 2020; 2020: 4730715. https://doi.org/10.1155/2020/4730715
- [48] Alqahtani RT. A model of effector–tumor cell interactions under chemotherapy: bifurcation analysis. Mathematics. 2025; 13(7): 1032. https://doi.org/10.3390/math13071032
- [49] Burrage K, Burrage PM, Kreikemeyer JN. Learning surrogate equations for the analysis of an agent-based cancer model. Front Appl Math Stat. 2025; 11: 1578604. https://doi.org/10.3389/fams.2025.1578604
- [50] Kim Y, Gilbert RM, Armstrong TS, Celiku O. Clinical outcome assessment trends in clinical trials contrasting oncology and non-oncology studies. Cancer Med. 2023; 12(16): 8715-26. https://doi.org/10.1002/cam4.6325

## **Appendix A**

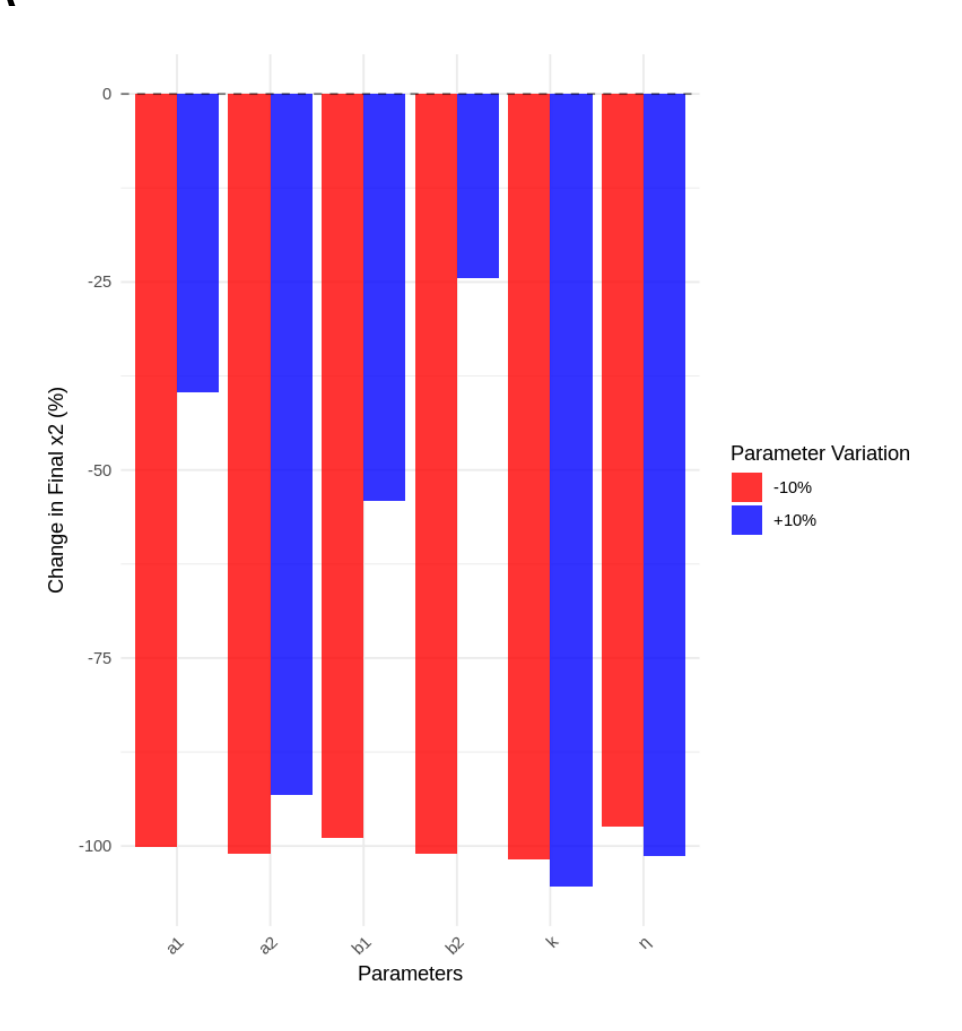


**Figure A:** Parameter Sensitivity Effect on Final Tumor Density  $(x_2)$